Environ Health Perspect

DOI: 10.1289/EHP6826

Note to readers with disabilities: *EHP* strives to ensure that all journal content is accessible to all readers. However, some figures and Supplemental Material published in *EHP* articles may not conform to 508 standards due to the complexity of the information being presented. If you need assistance accessing journal content, please contact ehp508@niehs.nih.gov. Our staff will work with you to assess and meet your accessibility needs within 3 working days.

Supplemental Material

In Vivo Characterization of the Toxicological Properties of DPhP, One of the Main Degradation Products of Aryl Phosphate Esters

Samia Selmi-Ruby, Jesús Marín-Sáez, Aurélie Fildier, Audrey Buleté, Myriam Abdallah, Jessica Garcia, Julie Deverchère, Loïc Spinner, Barbara Giroud, Sébastien Ibanez, Thierry Granjon, Claire Bardel, Alain Puisieux, Béatrice Fervers, Emmanuelle Vulliet, Léa Payen, and Arnaud M. Vigneron

Table of Contents

Figure S1. Retention time validation through analysis of chemical series.

Figure S2. MS/MS validation of annotated compounds.

Figure S3. Analysis of significant discriminating features for C1 and C3 samples.

Figure S4. Metabolic network analysis through structural identity and pathway mapping.

Figure S5. Hierarchical clustering of annotated features based on their median levels in each group of samples.

Figure S6. Correlation analysis between metabolic quantification obtained in positive mode.

Figure S7. Correlation analysis between metabolic quantification obtained in negative mode.

Figure S8. Gene ontology analysis of transcripts significantly dysregulated upon exposure to DPhP.

Figure S9. Protein interaction network based on significantly dysregulated genes upon exposure to DPhP.

Figure S10. Histological alterations induced by exposure to DPhP.

Additional File- Excel Document

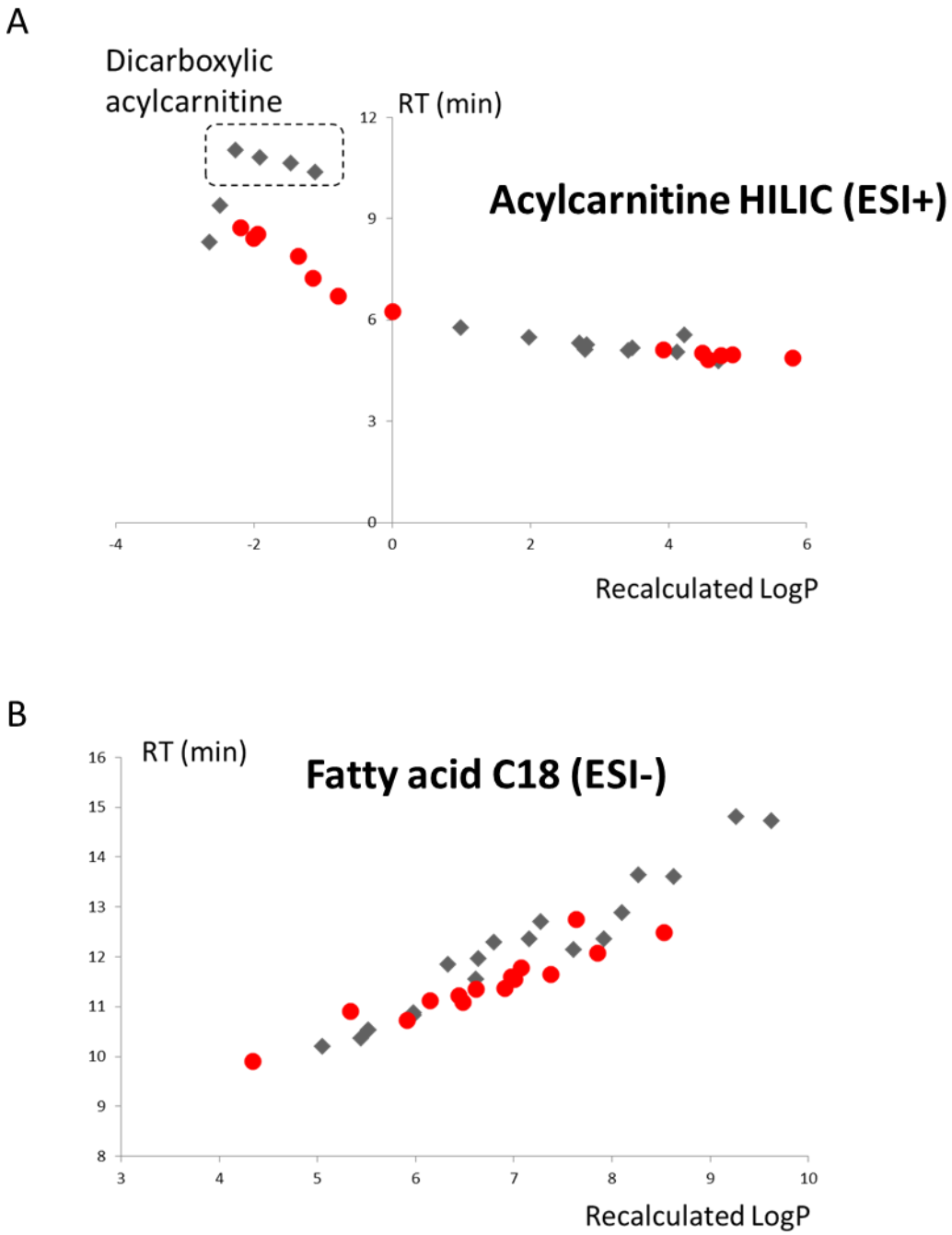

Figure S1. Retention time validation through analysis of chemical series

A. Dot plot representing the retention time by HILIC chromatography of annotated acylcarnitines according to their hydrophobicity (recalculated LogP = mean (LogD pH = 3.0, xLogP3). Red circles represent compounds validated by MS/MS fragmentation, whereas grey diamonds correspond to acylcarnitines only validated through their RT, m/z and known occurrence in biological fluids. Note that acylcarnitines with a second carboxylic acid function have shifted similarly to their annotation.

B. Similar dot plot presenting the annotated fatty acids separated by C18 chromatography.

A

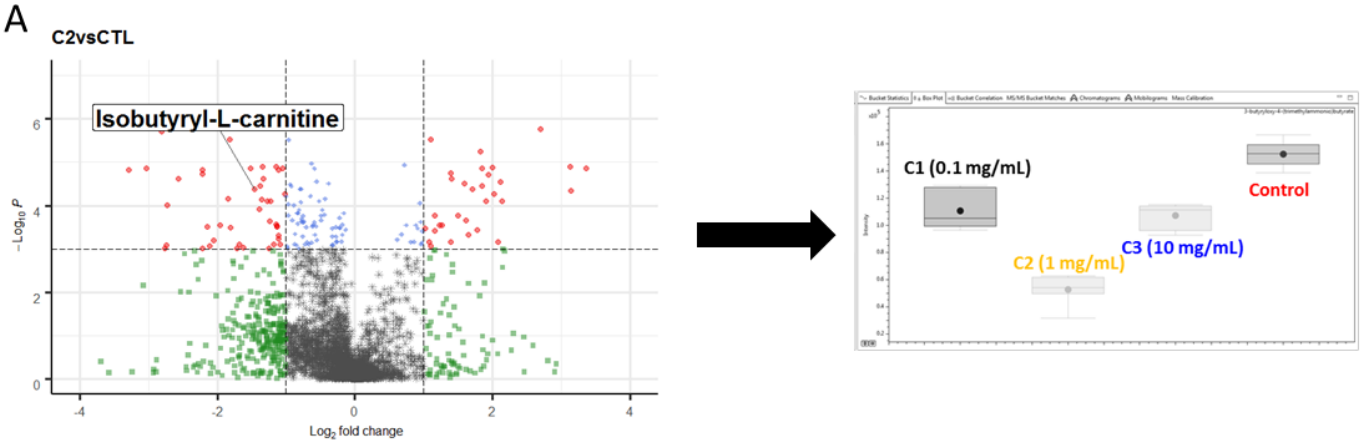

B

#	Neutral Formula	Ions	Ion Formula	M calc.	Ion	m/z m...	m/z calc.	rdb ...	eConf	Δ m/z [mDa]	Δ m/z [ppm]	mSigma	# Frag	IntCov. [%]
1	$C_{11}H_{21}NO_4$	▫	$C_{11}H_{22}NO_4^+$	231.1471	[M+H]+	232.1545	32.15433461	2.0	Even	-0.1565	-0.67	2.96	5	96.9
2	$C_{12}H_{17}N_5$	▫	$C_{12}H_{18}N_5^+$	231.1484	[M+H]+	232.1545	32.15367202	7.0	Even	1.1810	5.09	10.76	3	13.1
3	$C_9H_{21}N_5S$	▫	$C_9H_{22}N_5S^+$	231.1518	[M+H]+	232.1545	32.15904333	4.0	Even	4.5523	19.61	30.70	3	13.1
4	$C_7H_{17}N_7O_2$	▫	$C_7H_{18}N_7O_2^+$	231.1444	[M+H]+	232.1545	32.15164927	3.0	Even	-2.8418	-12.24	32.22	5	96.9

C

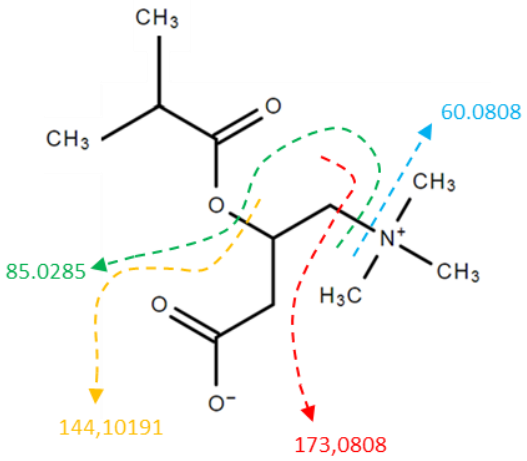

Isobutyryl-L-carnitine

D

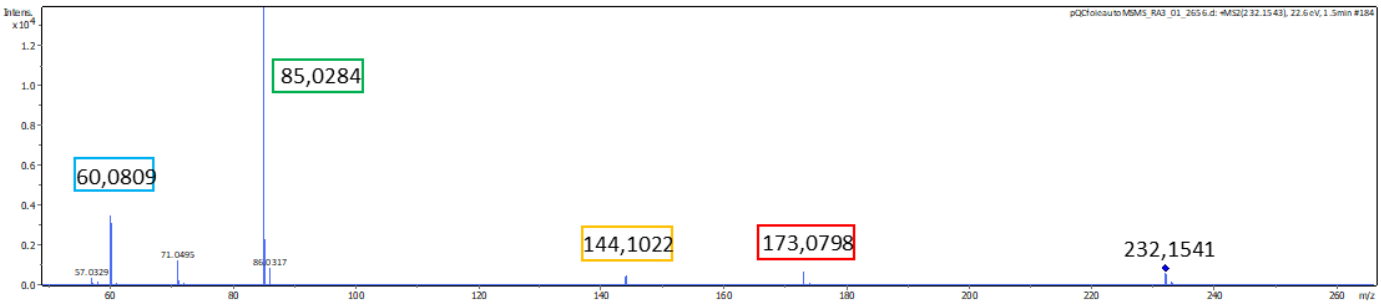

Figure S2. MS/MS validation of annotated compounds.

A. Signal intensities of the compounds were retrieved. A box and whisker plot could then be constructed to validate their higher or lower presence in exposed animals. An example is shown for isobutyryl-L-carnitine.

B. Compound annotation with some proposals of formulas. The first one corresponds to isobutyryl-L-carnitine.

C. An example of fragmentation prediction is shown for this same isobutyryl-L-carnitine

D. MS/MS experimental spectrum of isobutyryl-L-carnitine

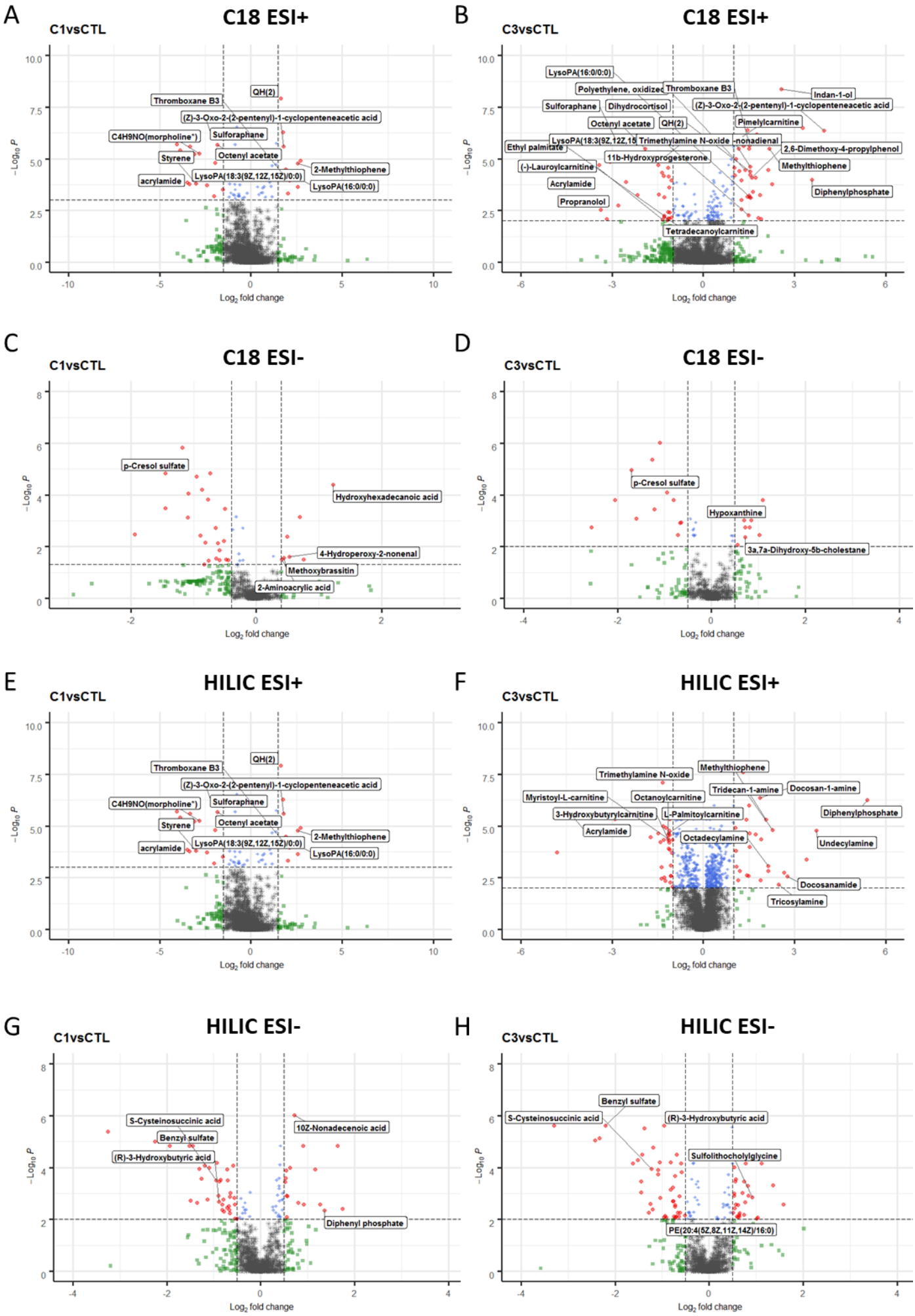
A
C18 ESI+
C1vsCTL
QH(2)
Thromboxane B3
(Z)-3-Oxo-2-(2-pentenyl)-1-cyclopenteneacetic acid
C4H9NO(morpholine+)
Sulforaphane
Styrene
Octenyl acetate
2-Methylthiophene
acrylamide
LysoPA(18:3(9Z,12Z,15Z)/0:0)
LysoPA(16:0/0:0)
B
C18 ESI+
C3vsCTL
LysoPA(16:0/0:0)
Polyethylene, oxidized
Thromboxane B3
Indan-1-ol
Sulforaphane
Dihydrocortisol
(Z)-3-Oxo-2-(2-pentenyl)-1-cyclopenteneacetic acid
Octenyl acetate
QH(2)
Pimelylcarnitine
Ethyl palmitate
LysoPA(18:3(9Z,12Z,15
Trimethylamine N-oxide
nonadienal
2,6-Dimethoxy-4-propylphenol
11b-Hydroxyprogesterone
(-)-Lauroylcarnitine
Methylthiophene
Acrylamide
Diphenylphosphate
Propranolol
Tetradecanoylcarnitine
C
C18 ESI-
C1vsCTL
p-Cresol sulfate
Hydroxyhexadecanoic acid
4-Hydroperoxy-2-nonenal
Methoxybrassitin
2-Aminoacrylic acid
D
C18 ESI-
C3vsCTL
p-Cresol sulfate
Hypoxanthine
3a,7a-Dihydroxy-5b-cholestane
E
HILIC ESI+
C1vsCTL
QH(2)
Thromboxane B3
(Z)-3-Oxo-2-(2-pentenyl)-1-cyclopenteneacetic acid
C4H9NO(morpholine+)
Sulforaphane
Styrene
Octenyl acetate
2-Methylthiophene
acrylamide
LysoPA(18:3(9Z,12Z,15Z)/0:0)
LysoPA(16:0/0:0)
F
HILIC ESI+
C3vsCTL
Methylthiophene
Trimethylamine N-oxide
Tridecan-1-amine
Docosan-1-amine
Myristoyl-L-carnitine
Octanoylcarnitine
Diphenylphosphate
3-Hydroxybutyrylcarnitine
L-Palmitoylcarnitine
Acrylamide
Octadecylamine
Undecylamine
Docosanamide
Tricosylamine
G
HILIC ESI-
C1vsCTL
S-Cysteinosuccinic acid
10Z-Nonadecenoic acid
Benzyl sulfate
(R)-3-Hydroxybutyric acid
Diphenyl phosphate
H
HILIC ESI-
C3vsCTL
Benzyl sulfate
S-Cysteinosuccinic acid
(R)-3-Hydroxybutyric acid
Sulfolithocholylglycine
PE(20:4(5Z,8Z,11Z,14Z)/16:0)
$-Log_{10}$ P
Log_2 fold change

Figure S3. Analysis of significant discriminating features for C1 and C3 samples

A. Volcano plots were created through observed median Fold change and adjusted p-value algorithm), comparing the metabolite level for the indicated groups (C1 or C3) quantified against control values, separated with C18 chromatography and quantified in positive mode. The most significant metabolites were annotated when possible and indicated directly on the plot. Cut-off for fold change/Adjusted P-value = 1.5/0.001 for (C1), 2/0.01 for (C3)

B. Similar analysis with metabolites quantified in negative mode. Cut-off for fold change/Adjusted P-value = 1.3/0.05 for (C1), 1.5/0.01 for (C3)

C. Similar analysis with metabolites separated with HILIC chromatography and quantified in positive mode. Cut-off for fold change/Adjusted P-value = 2/0.01 for (C1), 2/0.01 for (C3)

D. Similar analysis with the chromatography and the metabolites quantified in negative mode. Cut-off for fold change/Adjusted P-value = 1.5/0.01 for (C1), 1.5/0.01 for (C3)

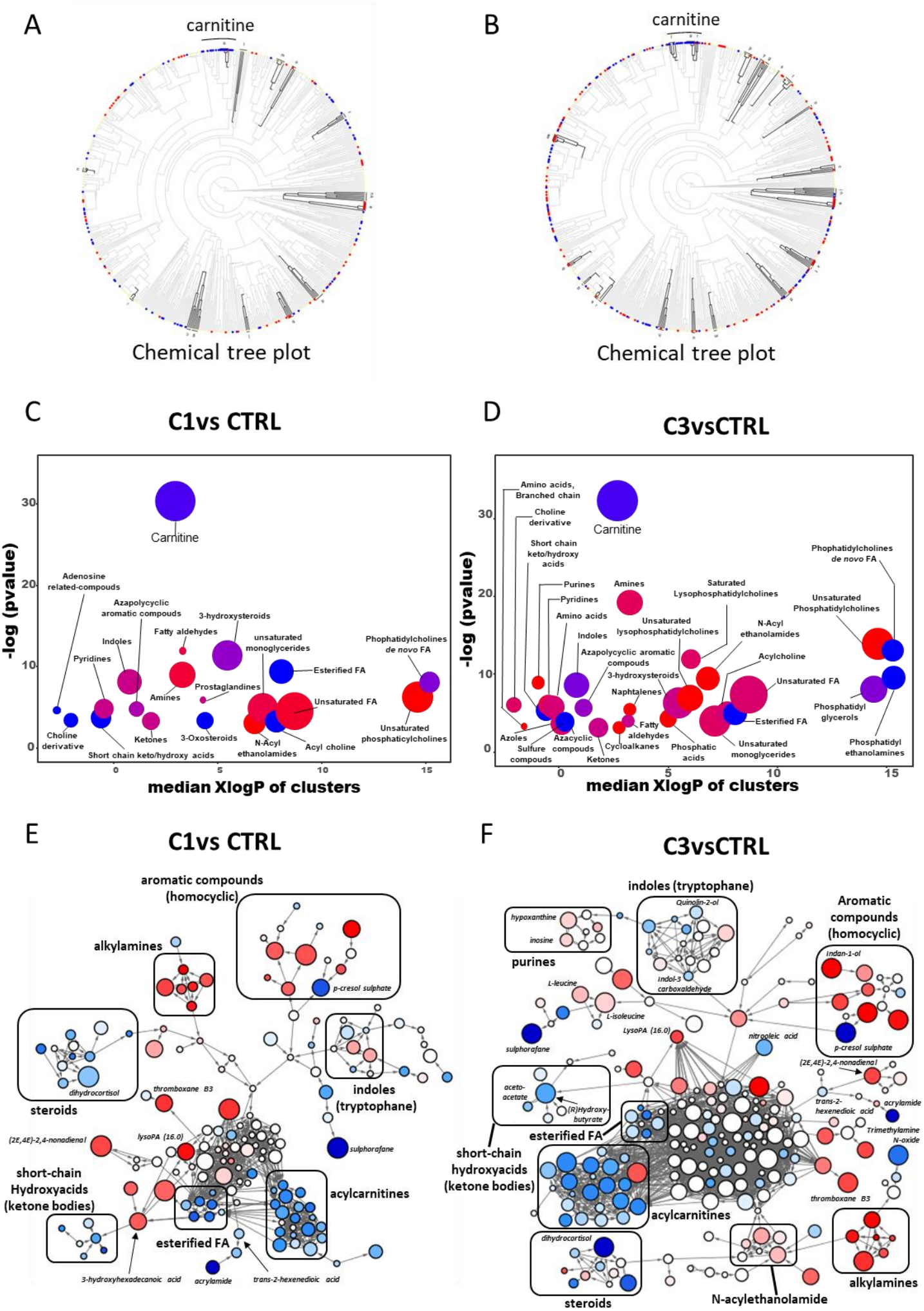
A
carnitine
Chemical tree plot
B
carnitine
Chemical tree plot
C
C1vs CTRL
-log (pvalue)
median XlogP of clusters
Carnitine
Adenosine related-compouds
Azapolycyclic aromatic compouds
3-hydroxysteroids
Fatty aldehydes
Indoles
Pyridines
unsaturated monoglycerides
Phophatidylcholines de novo FA
Esterified FA
Amines
Prostaglandines
Unsaturated FA
Choline derivative
Ketones
3-Oxosteroids
N-Acyl ethanolamides
Acyl choline
Unsaturated phosphaticylcholines
Short chain keto/hydroxy acids
D
C3vsCTRL
-log (pvalue)
median XlogP of clusters
Amino acids, Branched chain
Choline derivative
Carnitine
Short chain keto/hydroxy acids
Phophatidylcholines de novo FA
Purines
Amines
Saturated Lysophosphatidylcholines
Pyridines
Unsaturated Phosphatidylcholines
Amino acids
Unsaturated lysophosphatidylcholines
N-Acyl ethanolamides
Indoles
Azapolycyclic aromatic compouds
Acylcholine
3-hydroxysteroids
Unsaturated FA
Naphtalenes
Phosphatidyl glycerols
Esterified FA
Fatty aldehydes
Azoles
Azacyclic compouds
Cycloalkanes
Phosphatic acids
Unsaturated monoglycerides
Phosphatidyl ethanolamines
Sulfure compouds
Ketones
E
C1vs CTRL
aromatic compounds (homocyclic)
alkylamines
p-cresol sulphate
steroids
dihydrocortisol
thromboxane B3
indoles (tryptophane)
(2E,4E)-2,4-nonadienal
lysoPA (16.0)
sulphorafane
short-chain Hydroxyacids (ketone bodies)
acylcarnitines
esterified FA
3-hydroxyhexadecanoic acid
acrylamide
trans-2-hexenedioic acid
F
C3vsCTRL
indoles (tryptophane)
Quinolin-2-ol
hypoxanthine
inosine
purines
Aromatic compounds (homocyclic)
indan-1-ol
Indol-3 carboxaldehyde
L-leucine
L-isoleucine
LysoPA (16.0)
nitrooleic acid
sulphorafane
p-cresol sulphate
(2E,4E)-2,4-nonadienal
aceto-acetate
(R)Hydroxy-butyrate
trans-2-hexenedioic acid
acrylamide
esterified FA
Trimethylamine N-oxide
short-chain hydroxyacids (ketone bodies)
thromboxane B3
acylcarnitines
dihydrocortisol
alkylamines
steroids
N-acylethanolamide

Figure S4. Metabolic network analysis through structural identity and pathway mapping

A-B. Data associated with 635 annotated metabolites were used to perform a Chemical Similarity Enrichment Analysis (ChemRICH). A Tanimoto chemical similarity mapping form a clustered circular similarity tree. Dark black lines indicate boundaries of clusters that were significantly different in exposed animals at the indicated concentration versus control mice (P-value < 0.05). Higher metabolite levels in DphP-exposed mice (compared to those expose to vehicle) have been labelled as red nodes, lower levels have been marked in blue. The Acylcarnitine Cluster label has also been indicated.

C-D. ChemRICH set enrichment statistics plot of 635 metabolites extracted from exposed animals with the indicated concentration of DPhP versus control. Each node reflects a significantly altered cluster of metabolites. Enrichment P-values were obtained using the Kolmogorov-Smirnov test and median XlogP3 was calculated from individual values associated with each metabolite present in the cluster. Node size represents the total number of metabolites in each set of clusters. Continuous scale color for the nodes shows the proportion of fully increased (red) or fully decreased (blue) family of compounds in exposed mice compared to control mice. Nodes with an intermediate color (pink to purple) have both increased and decreased metabolites.

E-F. MetaMapp visualisation of the same metabolomics data highlighting the differential metabolic regulation and the organisation of metabolic clusters based on KEGG reactant pair information and Tanimoto chemical similarity matrix. Only metabolites significantly different (adjusted p-value < 0.05) were used to build the network. Metabolite levels that were higher in exposed mice have been labelled as red nodes ; those with lower levels have been marked in blue (continuous scale with white intermediate). P-values is encoded in node size (lowest p-value = highest size). Cluster are indicated. Metabolites previously clustered together based on their structural similarity could now be separated according to their different pathway mapping.

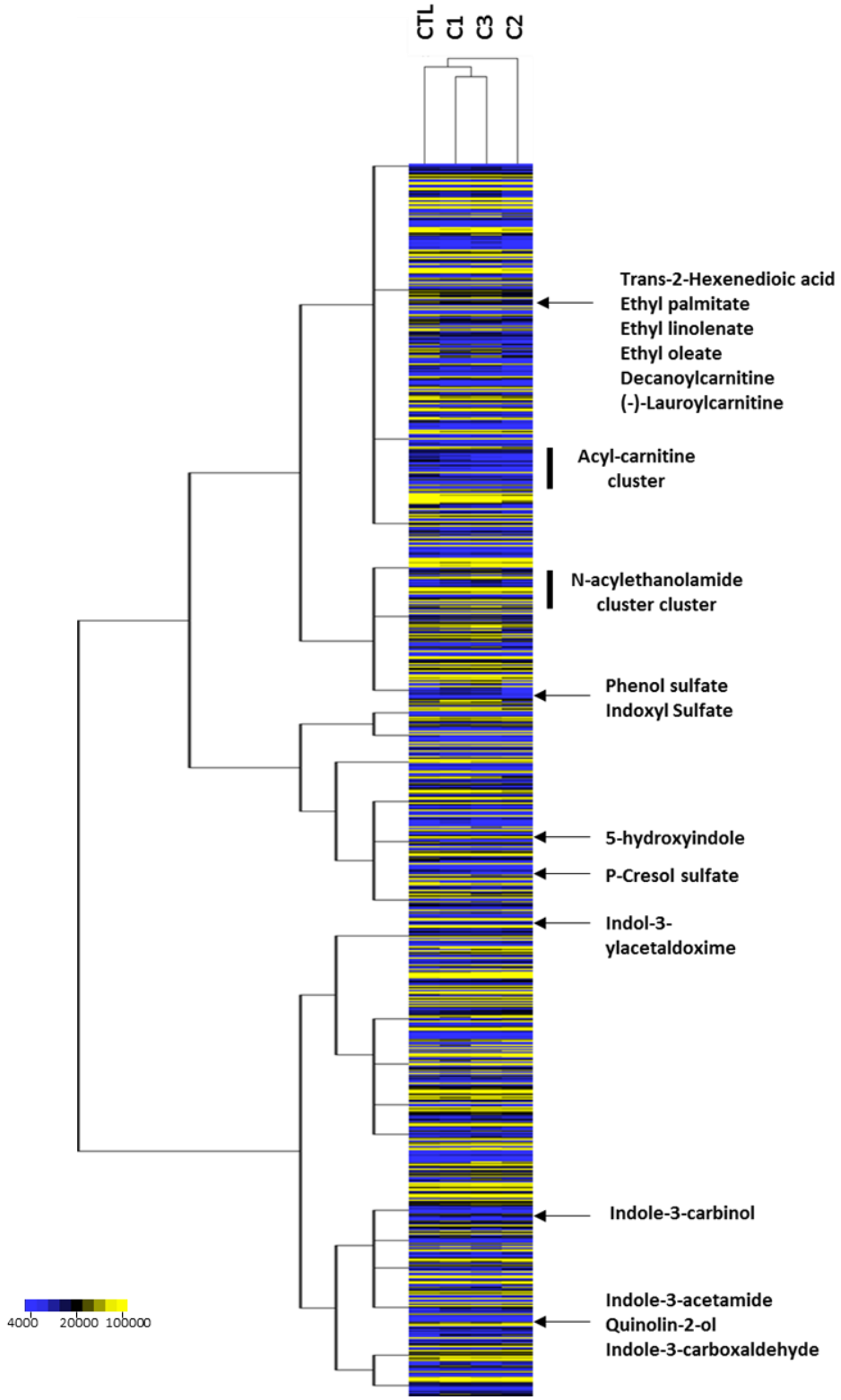

Figure S5. Hierarchical clustering of annotated features based on their median levels in each group of samples

633 metabolites represented by 876 features and the 4 groups of exposed and control animals were clustered hierarchically through their relative level (centroid linkage with spearman correlation). Features corresponding to the same metabolite present in different analytical procedure have been separated, explaining why a metabolite can appear several times in the Heatmap. Yellow-blue encoding is used to represent these metabolites according to their absolute amounts. Distance between levels of samples and metabolites are shown as two tree plots. Subclusters and a couple of compounds highlighted in the main manuscript or in the Figure 4 are indicated.

Correlation Plot

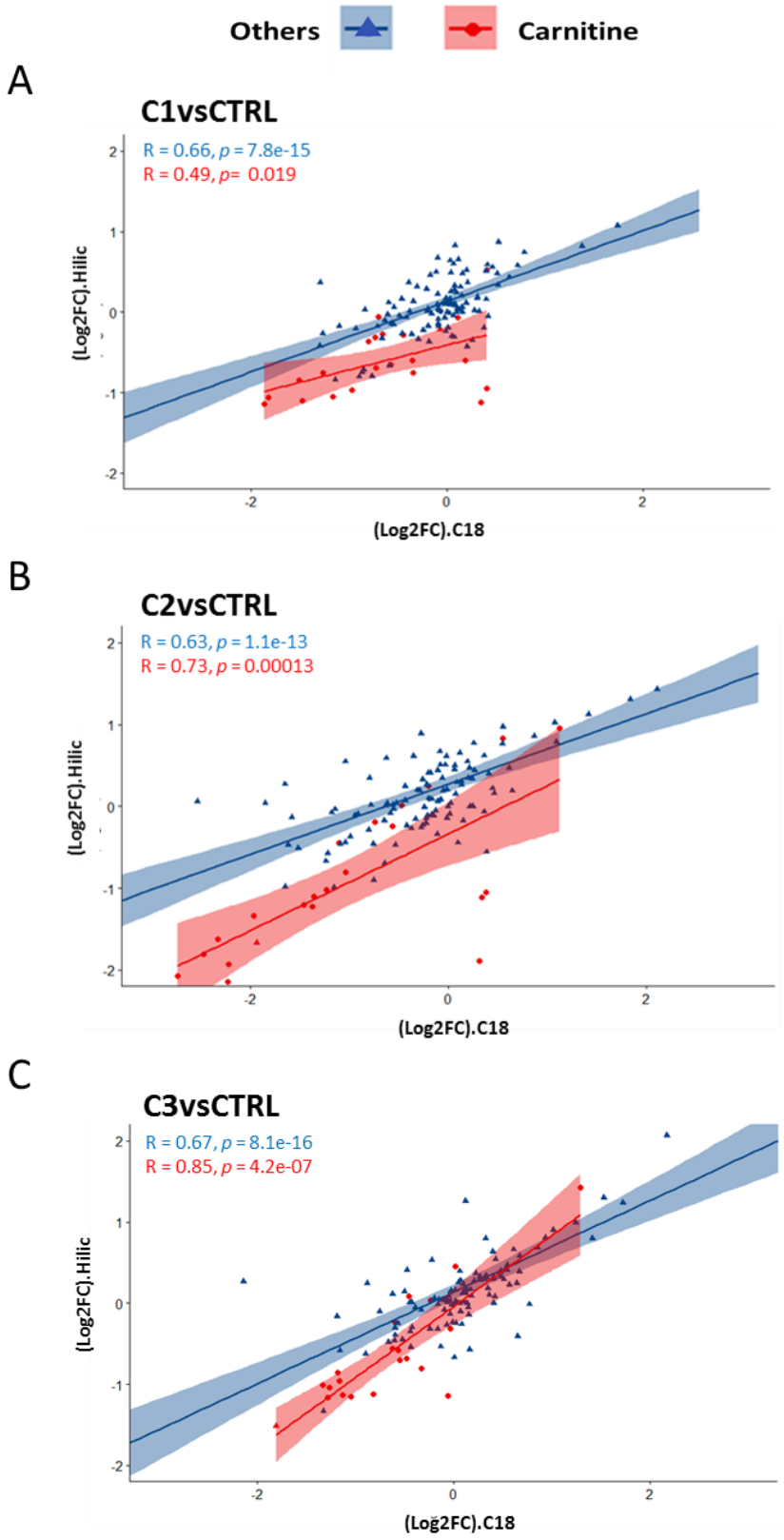

Figure S6. Correlation analysis between metabolic quantification obtained in positive mode

A-C. Correlation plots were created by comparing the observed fold changes of annotated metabolites quantified in both HILIC and C18 positive mode. Fold change corresponds to the difference of metabolite levels between the indicated group and control animals. A subcategory corresponding to acylcarnitine was extracted from other compounds. R coefficient correlation is indicated for bulk compounds and acylcarnitines.

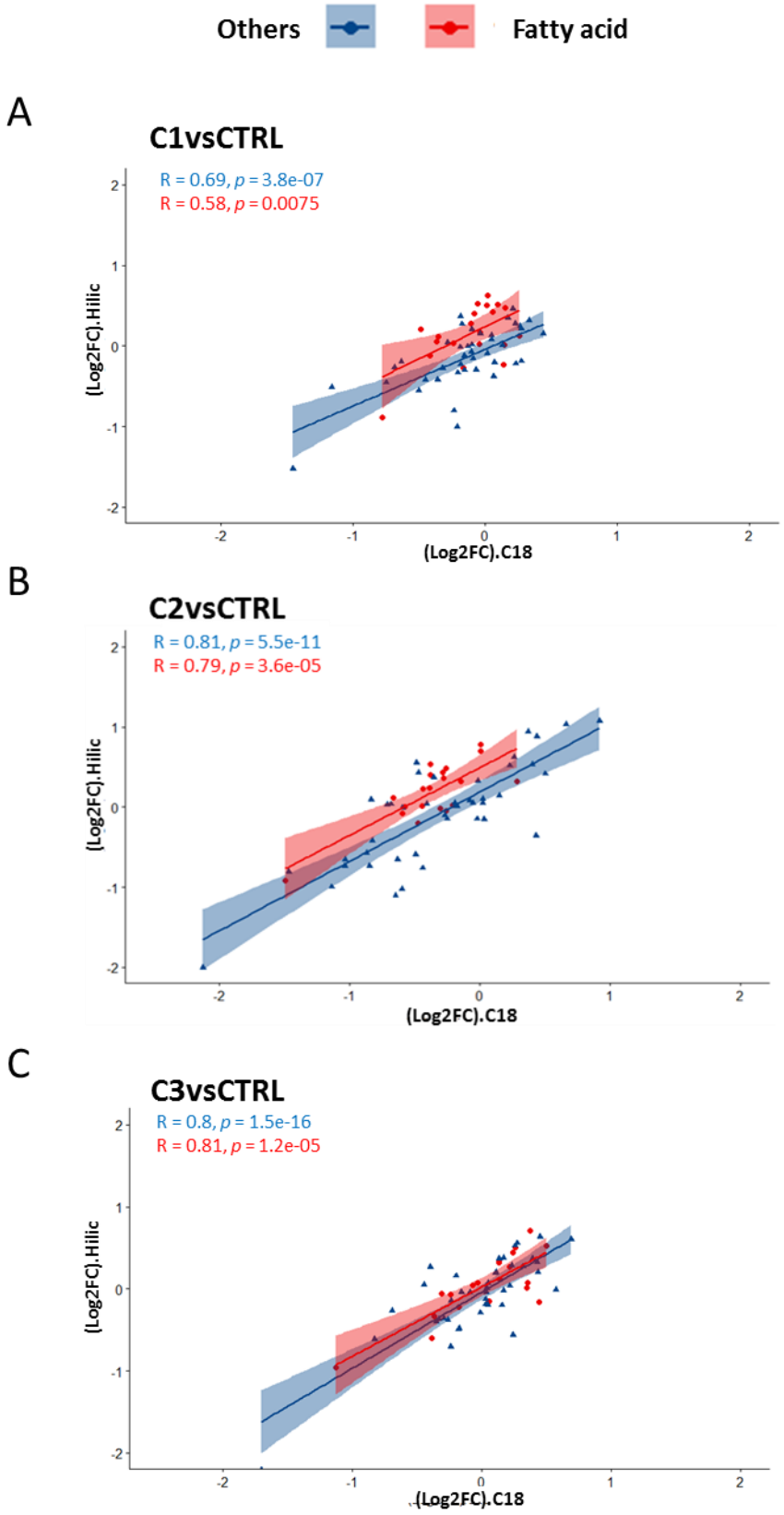

Figure S7. Correlation analysis between metabolic quantification obtained in negative mode

A-C. Correlation plots were created by comparing the observed fold changes of annotated metabolites quantified in both HILIC and C18 negative mode. Fold change corresponds to the difference of metabolite levels between the indicated group and control animals. A subcategory corresponding to fatty acids was extracted from other compounds. R coefficient correlation is indicated for bulk compounds and fatty acids

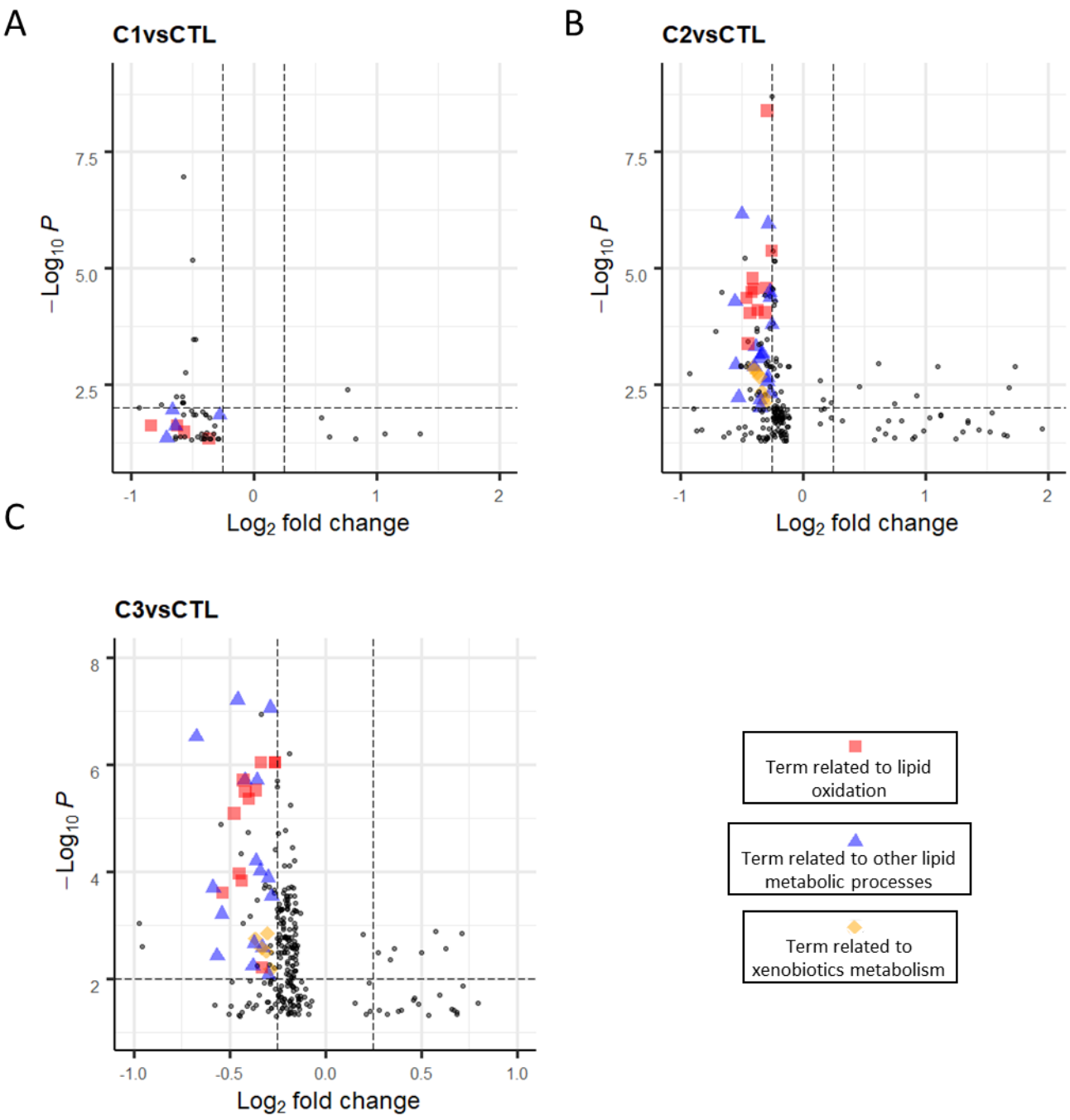

Figure S8. Gene ontology analysis of transcripts significantly dysregulated upon exposure to DPhP

A-C. Gene ontology analysis using the Log2 Fold Change of mRNA expression derived from animals exposed to the indicated concentration of DPhP vs control animals and performed through Functional Enrichment Analysis (© STRING Consortium 2019). Results are presented as a volcano plot of the significant discriminating functions. Terms related to lipid oxidation, lipid metabolic processes and xenobiotics metabolism are highlighted as indicated.

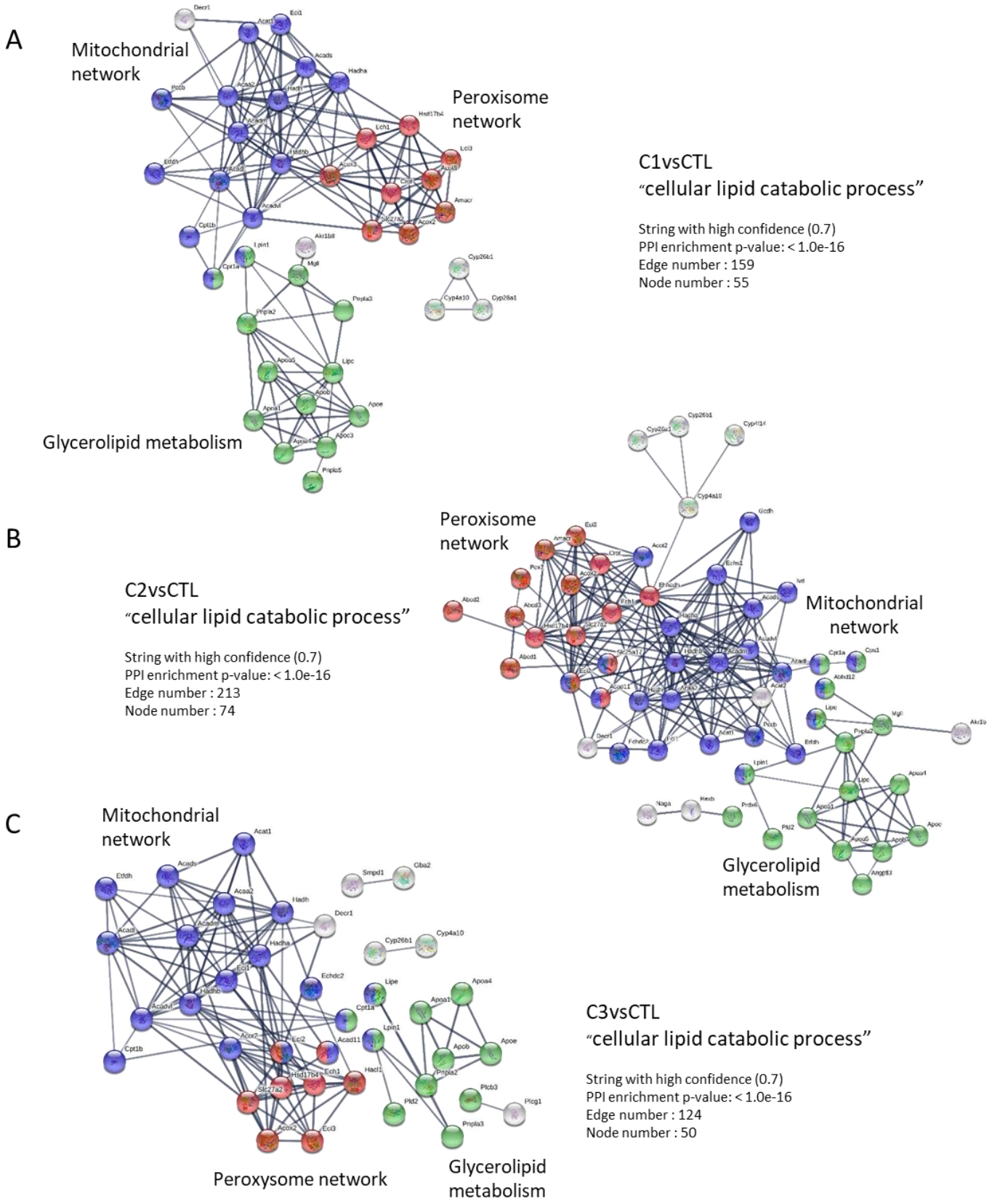

Figure S9. Protein interaction network based on significantly dysregulated genes upon exposure to DPhP.

A-C. Genes significantly dysregulated upon exposure to the indicated concentrations of DPhP and overlapping the indicated GO term were used to build a protein-protein interaction network (© STRING Consortium 2019) with a high level of confidence. Genes belonging to a particular network are highlighted in blue (Mitochondria), red (Peroxisome) or green (glycerophospholipid). Numbers of edges and nodes are indicated, as well as Protein-Protein-Interaction (PPI) enrichment (see methods).

A

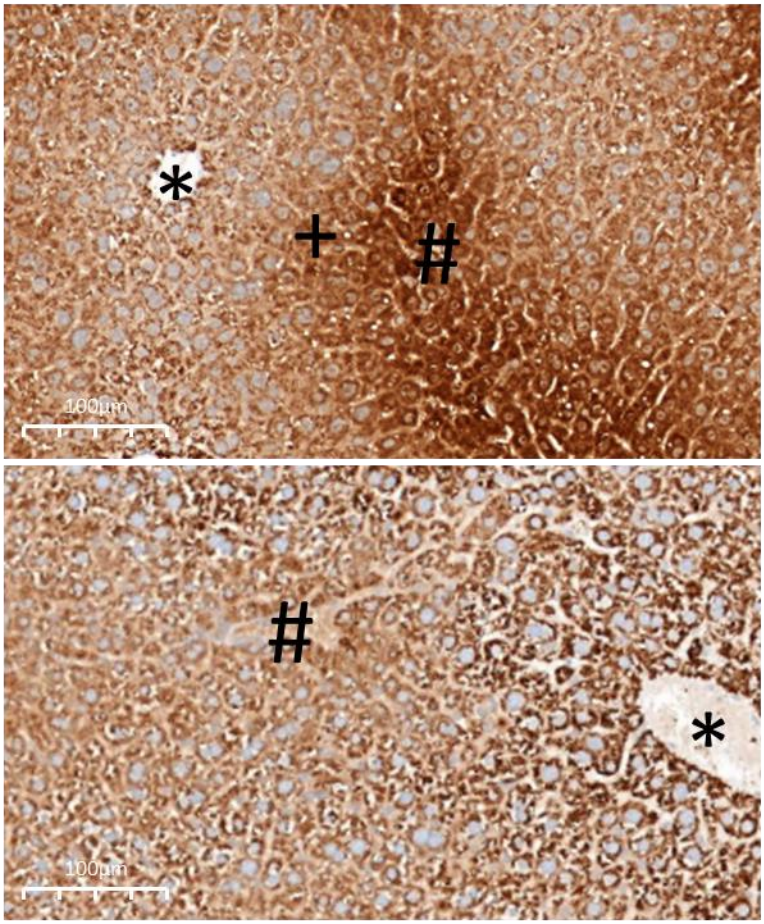

CTL

Hmgcs2

C3

B

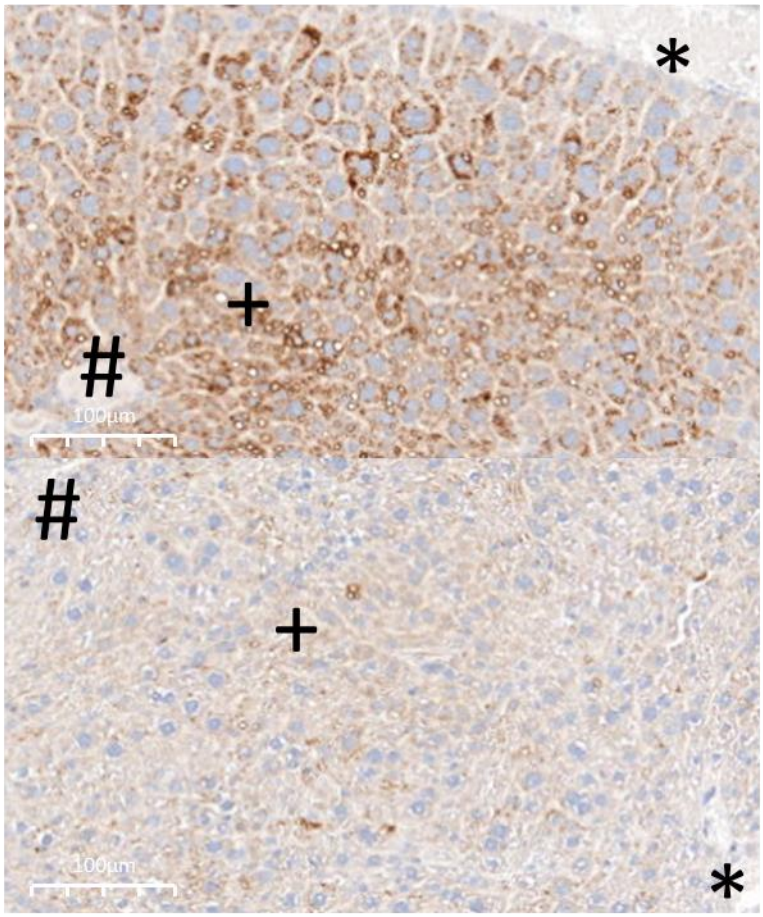

C2

Perilipin2

C3

Figure S10. Histological alterations induced by exposure to DPhP

A. Liver sections of mice exposed to the indicated concentrations of DPhP or a vehicle were immunostained with an antibody directed against Hmgcs2. Star, cross and hash denote the centrilobular, the intermediate and the portal area of the liver, respectively.

B. Liver sections of mice exposed to the indicated concentrations of DPhP or a vehicle were immunostained with an antibody directed against Perilipin 2. Star, cross and hash denote the centrilobular, the intermediate and the portal area or the liver, respectively.